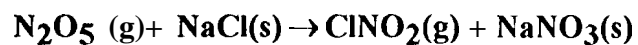


Heterogeneous Reactions of $\text{HNO}_3(\text{g}) + \text{NaCl}(\text{s}) \rightarrow \text{HCl}(\text{g}) + \text{NaNO}_3(\text{s})$ and



Ming-Taun Leu*, Raimo S. Timonen, Leon F. Keyser
Earth and Space Sciences Division
Jet Propulsion Laboratory
California Institute of Technology
Pasadena, CA 91109

Yuk L. Yung
Division of Geological and Planetary Sciences
California Institute of Technology
Pasadena, CA 91125

* Author to whom correspondence should be addressed.

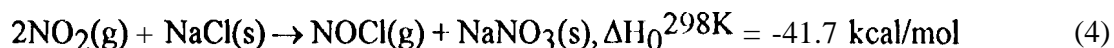
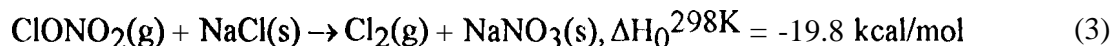
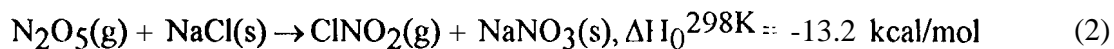
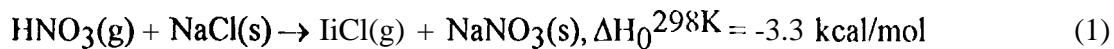
(submitted to the Journal of Physical Chemistry on).

Abstract

The heterogeneous reactions of $\text{HNO}_3(\text{g}) + \text{NaCl}(\text{s}) \rightarrow \text{HCl}(\text{g}) + \text{NaNO}_3(\text{s})$ (eq 1) and $\text{N}_2\text{O}_5(\text{g}) + \text{NaCl}(\text{s}) \rightarrow \text{ClNO}_2(\text{g}) + \text{NaNO}_3(\text{s})$ (eq 2) were investigated over a temperature range 223-296 K in a flow-tube reactor coupled to a quadrupole mass spectrometer. Either a chemical ionization mass spectrometer (CI MS) or an electron-impact ionization mass spectrometer (EIMS) was used to provide suitable detection sensitivity and selectivity. In order to mimic atmospheric conditions, partial pressures of HNO_3 and N_2O_5 in the range 6×10^{-8} - 2×10^{-6} Torr were used. Granule sizes and surface roughness of the solid NaCl substrates were determined by using a scanning electron microscope. For dry NaCl substrates, decay rates of HNO_3 were used to obtain $y(1) = 0.013 \pm 0.004$ (1σ) at 296 K and > 0.008 at 223 K, respectively. HCl was found to be the sole gas-phase product of reaction (1). The mechanism changed from heterogeneous reaction to predominantly physical adsorption when the reactor was cooled from 296 K to 223 K. For reaction (2) using dry salts, $y(2)$ was found to be less than 1.0×10^{-4} at both 223 K and 296 K. The gas-phase reaction product was identified as ClNO_2 in previous studies using an infrared spectrometer. An enhancement in reaction probability was observed if water was not completely removed from salt surfaces, probably due to the reaction of $\text{N}_2\text{O}_5(\text{g}) + \text{H}_2\text{O}(\text{s}) \rightarrow 2 \text{HNO}_3(\text{g})$. Our results are compared with previous literature values obtained using different experimental techniques and conditions. The implications of the present results for the enhancement of the hydrogen chloride column density in the lower stratosphere after the El Chichon volcanic eruption and for the chemistry of HCl and HNO_3 in the marine troposphere are discussed.

L Introduction

The heterogeneous reactions of solid sodium chloride with atmospheric trace gases, for example HNO_3 , N_2O_5 , ClONO_2 , and NO_2 ,



are of fundamental importance in atmospheric chemistry for the following reasons. First, it has been suggested that these reactions are responsible for the observed enhancement of the hydrogen chloride column density in the lower stratosphere after the El Chichon volcanic eruption. Second, reaction (1) can directly transform nitric acid into hydrogen chloride, which has been observed in the marine troposphere, resulting in a deficit of chloride in marine aerosols. Third, reactions (2)-(4) may be a potential source of reactive chlorine by converting solid sodium chloride into gaseous ClONO_2 , Cl_2 , and NOCl which undergo photodissociation processes to produce atomic chlorine. These chlorine atoms then react with methane or other molecules, producing HCl . It is now well established that an enhancement of the chlorine budget can influence the catalytic destruction of stratospheric ozone [1]. Therefore, it is important to investigate these reactions not only by measuring their reaction probabilities but also by identifying their reaction mechanisms, using experimental conditions as close as possible to the ambient environment.

Salt particles were collected by a crystal-balanced cascade impactor from the El Chichon volcanic clouds in the lower stratosphere in the spring of 1982 [2]. The number density was as much as $26 \text{ particles/cm}^3$ and the size was about 1-2 μm . Simultaneous measurements of the hydrogen chloride column density by a Fourier transform infrared spectrometer showed approximately a 40 % enhancement over the background observed

prior to the volcanic eruptions [3]. The observations of Mankin and Coffey [3] have recently been confirmed using the **decadal** record of **HCl** measurements taken at **Jungfraujoch** (Switzerland) by R. Zander [private communication, 1994]. The heterogeneous reactions (1)-(4) have been suggested to play an important role in these observations [4,5].

In the marine **boundary** layer, sea salt aerosols are generated by breaking waves on the ocean's surface. It has been observed that Na^+ is **often** in excess of Cl in aerosol samples, suggesting that sea salt reacts with NO_2 , N_2O_5 , HNO_3 or sulfate aerosols [6-9]. These reactions displace the chloride in aerosols and form **HCl**. In addition, reactions (2)-(4) may provide a source of atomic chlorine which removes **alkanes** and **dimethy** sulfide (**DMS**). This reaction mechanism has also been suggested to explain numerous atmospheric observations of gaseous nitric acid, **hydrochloric** acid, and nitrate particulate in the eastern U. S. [10], the greater Los Angeles **area** [11,12], and the Hawaiian islands [13].

There are several laboratory investigations of reactions (1)-(4). The reaction probability for (1) has been reported in a recent preliminary study [14] using X ray photoelectron spectroscopy to detect nitrate formation on **single** NaCl crystals in an ultrahigh vacuum chamber. This is a rather novel technique for surface reaction study, however, neither gaseous reactant nor gas-phase product was monitored in this study. Using a low-pressure flow reactor interfaced with a mass spectrometer, Fenter et al [15] determined γ for reaction (1) at 298 K. **HCl** was found to be the sole gas-phase product of the reaction. Internal surface areas were not considered in the determination of γ (1). It is somewhat surprising that these workers also obtained the same γ value for the uptake of HNO_3 on NaN_3 substrates.

Using an infrared spectrometer, Livingston and Finlayson-Pitts [16] determined a lower limit for γ (2). The initial concentration of N_2O_5 used in the reactor was 1.2×10^{14} molecules cm^{-3} , several orders of magnitude **greater** than the ambient concentration in the

troposphere. The ratio $[\text{HNO}_3]/[\text{N}_2\text{O}_5] = 0.55$ in the $\text{N}_2\text{O}_5/\text{air}$ mixtures was also measured. The reaction products were identified as ClNO_2 and HCl on the basis of their unique infrared spectra. The presence of the HNO_3 impurity may interfere with their study as discussed below. In a series of studies, Zetzsch and his coworkers [17-20] investigated the uptake of N_2O_5 by NaCl solutions from 262 to 278 K by using a droplet train technique. The experimental conditions used are more relevant to tropospheric conditions and the result is suitable for use in tropospheric modelling. Using a deposition profile measurement in an annular reactor and ion chromatography for nitrate analysis, Msibi et al. [21] obtained reaction probabilities for reaction (2) in both dry and wet NaCl substrates. The study requires a rather complicated procedure for the determination of γ .

For reaction (3), a summary of our work [22] using a fast flow-tube reactor interfaced to a quadrupole mass spectrometer has been recently published. Both the reactant decay and the product growth were used to determine the true reaction probability under stratospheric conditions. Reaction (4) has been shown to be too slow to be of importance in the atmosphere because it requires two NO_2 molecules simultaneously colliding on NaCl surface [23].

In this article, we report the measurement of reaction probabilities for reactions (1) and (2) using partial pressures of reactants about 6×10^{-8} to 2×10^{-6} Torr encountered in the lower stratosphere and also in the marine boundary layer. First, we will describe the experimental procedures used, including the details of the recently developed chemical ionization mass spectrometer. Next, we will summarize and discuss the results of the reaction probability measurements and a kinetic mechanism for reaction (1). Finally, we will compare our data with previous measurements and discuss briefly the atmospheric implications of our present results.

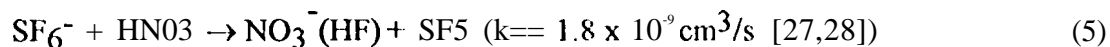
11. Experimental Section

The reaction probability measurement was performed in a fast flow-tube reactor coupled to a quadrupole mass spectrometer. Two detection systems, a chemical ionization mass spectrometer (CIMS) and an electron-impact ionization mass spectrometer (EIMS), were used depending upon the requirements of sensitivity and selectivity. The EIMS apparatus has been discussed in detail previously [24,25] and will not be repeated in this article. However, the CIMS apparatus has been recently developed in this laboratory and will be described as follows.

Flow Reactor/Chemical Ionization Mass Spectrometer. The neutral flow reactor was made of borosilicate glass, and its dimensions are 20.0 cm in length and 1.8 cm inside diameter (see Figures 1 and 2). The bottom of the reactor was recessed and made flat in order to hold the NaCl substrates in place. The depth of the recess is about 0.33 cm. The regulation of temperature was made possible by circulating cold methanol through the jacket surrounding the flow reactor and the temperature was measured by a thermocouple attached to the middle section. The pressure inside the reactor was monitored by a high-precision capacitance manometer which was located about 7 cm from the reactor at the downstream end. The measured pressure was corrected for the viscous pressure gradient between the measurement point and the midpoint of the reactor. The carrier gas was helium and was admitted to the reactor through a side-arm. The reactants, HN03 and N205, were added through a sliding borosilicate injector as shown in Figure 1. The average flow velocity in the neutral flow reactor was between 170 and 2800 cm/s. A large glass valve located at the downstream end of the neutral reactor was used to regulate the flow velocity.

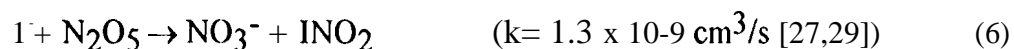
A schematic diagram of the CIMS apparatus is shown in Figure 1. The design is similar to that used previously [26]. The ion flow reactor was constructed of a stainless steel tube of 127 cm in length and 7.0 cm inside diameter. A large flow of helium, 6-10 slpm (standard liter per minute at 293 K), was passed through the reactor at a constant

pressure in the range of 0.2 to 0.5 Torr. A large capacity booster pump (Edwards High Vacuum, Model EH2600, 610 I/s) was used to evacuate the ion flow reactor. The average flow velocity used in the ion flow reactor was typically about 100-160 m/s in these experiments. A small flow of SF₆, 1-5 sccm (standard cubic centimeter per minute at 293 K), was mixed with the helium carrier and SF₆⁻ ions were formed by electron attachment. The electrons were produced by passing a current (6 - 10 A) through a filament located at a side-arm port of the reactor. The filament material was tungsten, rhenium, or thoriated iridium. SF₆⁻ ions were allowed to react with the trace gas species from the neutral flow reactor, for example, HN03 by the reaction



These ions were then effused through a molybdenum orifice (0.5 mm in diameter) and collimated by a set of ion lenses. The first lens was separated from the molybdenum orifice about 0.5 cm and was biased by a small voltage (1 -10 V) in order to focus the ions through the lens system. A quadrupole mass spectrometer (a set of quadrupole rods 9 inches in length and 5/8 inch in diameter powered by a C-60 electronics module) was used to analyze these ions (for example, 146 amu for SF₆⁻ and 82 amu for NO₃⁻(HF)). The ions were amplified by a conversion dynode/electron multiplier and then recorded by an electrometer (Extrel Corp., Model 031-2). A mini-computer was used to acquire the data for further analysis. The calibration of HN03 signals is shown in Figure 3. The dynamic range is linear up to $3 \times 10^{11} \text{ molecules/cm}^3$ (or $1 \times 10^{-5} \text{ Torr}$). The detection sensitivity for HN03 using this technique is about $2 \times 10^8 \text{ molecules/cm}^3$ (or $6 \times 10^{-9} \text{ Torr}$ and S/N= 1 for 1 s integration). The detection sensitivity is more than adequate for the present experiment. Further improvement is possible by using a new electron multiplier.

The detection of N2O5 in the presence of HNO3 was performed in the same manner. The reagent ions I^- were generated from the dissociative attachment of CF_3I by electrons. The detection of I^- was made by using the reaction



The rate coefficient for reaction (6) is several orders of magnitude greater than that for the $I^- + HNO_3 \rightarrow NO_3^- + HI$ reaction [27]. Thus, it is possible to detect N2O5 selectively in the presence of HNO3. The calibration of N2O5 signals is shown in Figure 4. The dynamic range is also linear up to $3 \times 10^{11} \text{ molecules/cm}^3$ (or $1 \times 10^{-5} \text{ Torr}$). Currently, the detection limit for N2O5 is about $1 \times 10^8 \text{ molecules/cm}^3$ (or about $3 \times 10^{-9} \text{ Torr}$ and $S/N = 1$ for 1 s integration) using this CIMS apparatus. Again, the selective detection of N2O5 is adequate for this experiment.

Synthesis of HNO₃ and N₂O₅. HNO₃ was prepared by reacting H₂SO₄ (96 wt% purity liquid) with reagent grade NaNO₃ (99 %purity solid) in vacuum and the nitric acid vapor was collected in a Pyrex vessel at liquid nitrogen temperature. The HNO₃ thus prepared was further purified by vacuum distillation at 195 K. N₂O₅ was prepared by mixing NO₂ with an excess of O₃ from an ozonizer. The N₂O₅ was stored at 195 K before use. The HNO₃ impurity in N₂O₅ was checked by CIMS and was found to be less than 10 %. The interference of this impurity in the detection of N₂O₅ is negligible as discussed in the previous paragraph.

Preparation of the NaCl Substrates. NaCl crystals Q-99.8 % purity, analytical reagent) were supplied by J. T. Baker, Inc. The impurity levels of bromine or iodine compounds, which may react with HNO₃ or N₂O₅, were stated to be less than 0.005% and 0.001%, respectively. The size and shape of these crystals were examined by using a scanning electron microscope and the typical shape of the NaCl particles is cubic and the average size is about 0.44 μm. The BET specific surface area of these samples was found

to be about 100 (+100, -50) cm^2/g . The specific surface area, S_g , was also calculated from the average crystal size by using the following equation[30]

$$S_g = 6/\rho_t d \quad (7)$$

where ρ_t is the true density of NaCl (2.165 g/cm^3) [31] and d is the particle size. Using $d = 0.44$ mm obtained from the SEM experiments, we obtain a surface area of 62 cm^2/g from eq 7 which is in agreement with the BET surface area within the stated experimental error.

The NaCl substrates were prepared in such a way to simulate the aerosol conditions encountered in the stratosphere after a volcanic eruption. In one set of the experiments the granules were baked at temperatures up to 473 K in the flow reactor overnight; the H₂O vapor pressure over these substrates was measured to be less than 2×10^{-5} Torr using the EIMS apparatus. In another set of the experiments, the granules were held in flow reactor and a stream of H₂O vapor was passed over the NaCl granules; the H₂O vapor pressure was kept in the range, 2×10^{-5} - 2×10^{-4} Torr. The temperature of the NaCl substrates inside the reactor was regulated between 223 K and 296 K. The thickness of the NaCl substrates inside the reactor was varied from 1.0 mm to 4.0 mm. Thus, the number of granule layers for the NaCl substrates is about 2 to 9.

Some experiments were performed using solid sodium chloride crystals which were supplied from Solon Technologies, Inc. These crystals were polished and cleaved in the (100) plane. Their dimensions are 25 mm x 12 mm x 2 mm. They were spread at the bottom of the flow reactor. It is reasonable to assume that only the geometric area of these crystals is available for reaction with HNO₃.

Procedures for Reaction Probability Measurements. The reaction probabilities for (1) and (2) were determined as follows. The loss rates of HNO₃ and N₂O₅ were measured as a function of inlet position, z . The reaction time was calculated by using $t =$

z/v where v is the average flow velocity. In each experiment we calculated the cross sectional area of the reactor and then the flow velocity. The first-order rate constant, k_s , was calculated from the slope of a linear least-squares fit to the experimental data. The axial gas-phase diffusion correction for k_s was made by using the following equation [32,33]

$$k_g = k_s (1 + k_s D / v^2) \quad (8)$$

The diffusion coefficient of HN03 and N_2O_5 in helium were estimated to be $pD = 495$ Torr cm^2s^{-1} and 350 Torr cm^2/s at 296 K, respectively[34]. A temperature coefficient of $T^{1.76}$ for the diffusion coefficient was also assumed. The rate corrected for gas-phase diffusion is designated as k_g .

For radial gas-phase diffusion, it is more difficult to estimate the correction to k_s because the reactor is no longer a fully symmetric cylindrical tube. If we use the full reactor radius of 0.9 cm in the calculation, the correction is relatively small, less than 10 %. Since this correction is not precise, we neglected it in the data analysis.

Based on the geometric area, S , of the NaCl substrate and the volume, V , of the reactor, the reaction probability, γ_g , was then calculated by using the following equation [35,36]

$$\gamma_g = 4k_g V / \bar{w} S \quad (9)$$

where \bar{w} is the average molecular velocity for HN03 and N_2O_5 . Note that this equation is valid for $\gamma_g < 0.1$ only, which holds for the present experiments.

To account for the surfaces of the salt granules beneath the top layer, we used an analysis recently developed and successfully applied to heterogeneous reactions on porous

ice films [35,36]. We model the NaCl substrate as hexagonal close-packed (HCP) spherical granules stacked in layers. For this model, the following equation holds

$$\gamma_t = \gamma_g \pi^{-1} 3^{1/2} \{1 + \eta[2(N_L - 1) + (3/2)^{1/2}]\}^{-1} \quad (10)$$

where γ_t is the true reaction probability for reactions (1) and (2), and N_L is the number of granule layers or the ratio of the thickness of the NaCl substrates to the average granule size. In eq 5, η is the effectiveness factor, which is the fraction of the NaCl surface that participates in the reaction. This factor is determined by the relative rates of pore diffusion to surface reaction and is given by

$$\eta = \phi^{-1} \tanh \phi \quad (11)$$

$$\phi = (h/d)[3\rho_b/2(\rho_t - \rho_b)] (\tau\gamma_t)^{1/2} \quad (12)$$

where h is the substrate thickness, d is the average size of granules, ρ_b is the bulk density, ρ_t is the true density and τ is a tortuosity factor. Typically, this factor is between 1.7 and 4 [37]. In our data analysis, we used a value of 2. This type of calculation has been used and discussed in previous publications [22,24,25].

In general, the magnitude of the corrections that convert γ_g to γ_t is less than a factor of 3 for $\gamma_t > 0.1$. However, for $\gamma_t < 0.1$, the corrections become much larger [35,36]. The possible uncertainties in the correction factors can be estimated by assessing the expected errors introduced by uncertainties in N_L , τ , and the type of packing (bulk density). For an uncertain in N_L of ± 2 within the range used, the errors in the correction factors are less than 1 So/O. For $\tau = 2$ or 3 [37], the error in the correction factors is less than $\pm 20\%$. For layer packing between simple cubic packing (SCP) and HCP, the correction factor error ranges over $\pm 25\%$. Including the errors (~ 15 -25%)

associated with the measurements of temperature, total pressure, flow rates and external gas-phase diffusion correction, we estimate the **systematic** error is about a factor of 2.

111. Results

$\text{HNO}_3 + \text{NaCl} \rightarrow \text{HCl} + \text{NaNO}_3$ (1). The uptake of HNO_3 in the presence of baked NaCl substrate at 296 K is shown in Figure 5(a). This experiment was performed using the EIMS apparatus and both HNO_3 and HCl were monitored using 46 amu and 36 amu, respectively. The Pyrex injector was moved upstream and downstream of the flow-tube reactor in this series of experiments. The experimental conditions used were: $m(\text{NaCl}) = 5.0 \text{ g}$, $p(\text{total}) = 0.308 \text{ Torr}$, $v = 1051 \text{ cm/s}$, and $p(\text{HNO}_3) = 6.7 \times 10^{-7} \text{ Torr}$. The reaction product, HCl , was produced readily and its yield was found to be near unity. To test the surface deactivation, another experiment was performed in a much longer reaction time (shown in Figure 5(b)). The experimental conditions were $m(\text{NaCl}) = 5.0 \text{ g}$, $p(\text{total}) = 0.343 \text{ Torr}$, $v = 1276 \text{ cm/s}$ and $p(\text{HNO}_3) = 1.7 \times 10^{-6} \text{ Torr}$. It is intriguing to note that the NaCl surface is not completely saturated even after three hours of exposure of HNO_3 and the amount of HNO_3 uptake ($> 1.1 \times 10^{15} \text{ molecules/cm}^2$) is greater than one monolayer ($\sim 6 \times 10^{14} \text{ molecules/cm}^2$). It is possible that during the reaction, the NaCl surface may form microcrystallites of NaNO_3 , regenerating fresh NaCl surfaces for further reaction. In other words, the crystal lattice of NaCl may be ruptured during the reaction. Another possibility is the diffusion of nitric acid through the solid salts. This type of the uptake behavior is consistent with our previous work on the uptake of ClONO_2 by NaCl substrates.[22]

A similar experiment was also carried out at a temperature of 223 K and the result is shown in Figure 6(a). The experimental conditions were $m(\text{NaCl}) = 5.0 \text{ g}$, $v = 1120 \text{ cm/s}$, $p(\text{total}) = 0.321 \text{ Torr}$ and $p(\text{HCl}) = 1.8 \times 10^{-6} \text{ Torr}$. In addition to heterogeneous reaction (1) there was a marked physical adsorption of HNO_3 on the NaCl surface. Furthermore, the surface was deactivated rapidly within about 10 minutes, much shorter than that in the experiment at 296 K. By pushing the injector back to the original position and allowing the warm Pyrex injector to anneal the substrates, the amount of HNO_3 desorbed was about 90-95% of the HNO_3 uptake. Nonetheless, the HCl yield

(about 5-10 % of the HN03 uptake) is much smaller than that at 296 K. The rapid surface deactivation effect may interfere with the determination of the value which will be discussed later.

To test this hypothesis, we also performed an experiment on the physical uptake of HN03 on NaN03 solid. The result is shown in Figure 6(b). A similar kinetic behavior as shown in Figure 6(a) was observed. The resorption peak was always smaller than the adsorption peak, suggesting some of HN03 may stay on the surface. Furthermore, no reaction product is found in this experiment.

For an irreversible pseudo-first-order reaction under plug-flow conditions, the decay of HN03 is given by the equation [22,25]

$$\ln[S(z)] = -k_s(z/v) + \ln[S(0)] \quad (13)$$

where $S(z)$ is the HN03 signal when the injector is at z , $S(0)$ is the signal when the NaCl is bypassed, and z/v is the reaction time. The observed rates, k_s , are determined from the slopes of linear-least-squares fits to these data.

Typical data of the HN03 loss as a function of injector position at 295 K are shown in Figure 7. The CIMS apparatus was used for the detection of HN03 in this experiment. The experimental conditions were $m(\text{NaCl}) = 22 \text{ g}$, $v = 2738 \text{ cm/s}$ and $p(\text{HNO}_3) = 7.9 \times 10^{-8} \text{ Torr}$. The salts were baked overnight in vacuum before use. In the absence of the NaCl substrates, the HN03 signals are independent of the injector position, providing evidence that the physical adsorption of HN03 on the surfaces of the flow-tube reactor was negligible, consistent with the data shown in Figure 5. With NaCl present, the decay of the HN03 signals was linear according to eq (13) which suggests that the pseudo-first-order condition is valid. The rate determined as the injector was pulled-out (from downstream to upstream) is nearly identical to that when the injector was

pushed-in (from upstream to downstream). Using the procedures discussed in a previous section, an average value of $\gamma(1) = 0.015$ was obtained.

A similar experiment was also performed at 223 K and the result is shown in Figure 8. The experimental conditions used were $m(\text{NaCl}) = 20$ g, $v = 1728$ cm/s, and $p(\text{HNO}_3) = 6.9 \times 10^{-8}$ Torr. The NaCl substrates were baked overnight in vacuum. It is evident that the rate observed when the injector was moved from downstream to upstream is smaller than that observed when the injector was moved from upstream to downstream because of the adsorption/desorption processes of HNO_3 occurring on the NaCl surface. A value of $y = 0.005$ was determined only from the data when the injector was moved from downstream to upstream and this should represent a lower limit for reaction(1) at 223 K. A weak signal of HCl was also observed, possibly due to the adsorption of HCl on the NaCl surface.

The experimental conditions used in the determination of the reaction probabilities for (1) are summarized in Table 1. Initial HNO_3 pressures were varied from 6.5×10^{-8} to 1.1×10^{-6} Torr and the temperature from 223 K to 296 K in these experiments. The γ values are approximately independent of the NaCl preparation (baked, unbaked, or water vapor added). The average value is 0.0133 ± 0.004 at 296 K and >0.008 at 223 K, respectively. The error quoted is one standard deviation. It is of interest to note that the uptake coefficients apparently depend on $p(\text{HNO}_3)$ used because of the surface deactivation. For example, the data collected at lower reactant pressures at room temperature is about a factor of 2 greater than that using larger reactant pressures as registered in Table 1. Several preliminary experiments were performed using much larger HNO_3 pressures about $(1-3) \times 10^{-5}$ Torr, γ values were found to be about 0.0004 at 296 K, much smaller than that listed in Table 1. Apparently, surface saturation plays an important role in these measurements.

A few experiments were performed by placing seven pieces of single crystals (25 mm x 12 mm x 2 mm) at the bottom of the flow reactor. The crystals were evacuated for

a few hours at 296 K. We carried out the experiment in the same manner as the powder substrates using a partial pressure of HN03 about 2.5×10^{-6} Torr and obtained a value of $\gamma = (2.4 \pm 0.6) \times 10^{-3}$. Because of smaller surface area available for reaction, the deactivation is rather serious during the reaction time of 10-20 s. Thus, this γ value should be considered as a lower limit for (1).

$\text{N2O5} + \text{NaCl} \rightarrow \text{ClNO}_2 + \text{NaNO}_3$ (2). The reaction probability for (2) has been measured in a similar manner as that for (1). Typical data are shown in Figure 9. The experimental conditions were $m(\text{NaCl}) = 20 \text{ g}$, $p(\text{total}) = 1.346 \text{ Torr}$, $v = 518 \text{ cm/s}$, $T = 296 \text{ K}$, and $p(\text{N}_2\text{O}_5) = 2.1 \times 10^{-6} \text{ Torr}$. The salts were not baked, but evacuated in vacuum for a couple of hours. The N2O5 signals using the CIMS apparatus were monitored as a function of the sliding injector position in the presence and absence of the NaCl substrates. The uptake of N2O5 on the Pyrex surface is negligible. A value of $\gamma(2) = 3 \times 10^{-4}$ was obtained on the basis of the loss rate of N2O5 signals. In other experiments for baked NaCl substrates, the decay rates, k_s , were always smaller than 10 s^{-1} . Using the procedures discussed in the previous section, $\gamma(2)$ was found to be less than 1×10^{-4} at both 223 K and 296 K for dry NaCl substrates. For unbaked salts, $\gamma(2)$ is slightly enhanced, probably due to the reaction of $\text{N}_2\text{O}_5 + \text{H}_2\text{O} \rightarrow 2 \text{HNO}_3$ on salt surfaces followed by reaction (1). These results are summarized in Table 2.

IV. Discussion

In this article we report $\gamma(1) = 0.013 \pm 0.004$ at 296 K and >0.008 at 223 K, respectively, using a fast flow-reactor coupled to a quadrupole mass spectrometer. HCl is the sole gas-phase product of reaction (1). In addition, an upper limit of 1.0×10^{-4} for $\gamma(2)$ in the temperature range 223-296 K was also determined for dry NaCl granules. An enhancement in reactivity was also measured for slightly wet salts, apparently due to the reaction of $\text{N2O5} + \text{H2O} \rightarrow 2 \text{HN03}$ on the NaCl surfaces. In Table 3 we compare our present results with literature values.

Comparison with Previous Measurements.

Using X ray photoelectron spectroscopy to follow the formation of nitrate on the surfaces of single crystals of NaCl, Laux et al.[14] obtained a value of $y(1) = (4 \pm 2) \times 10^{-4}$ at 298 K, which is about a factor of 30 smaller than our data summarized in Table 1. Also, their value is much smaller than our lower limit data using single NaCl crystals. In their study no gas-phase products were reported. The NaCl crystals were placed in an ultrahigh vacuum chamber; thus the surface should be free of significant amounts of water. Since the surface areas of the NaCl crystals were very smooth (single crystals were used), it is likely that significant surface saturation took place in their experiments. Therefore, the observed y value should be considered as a lower limit.

Rossi and his coworkers [15] investigated the uptake of nitric acid by solid salts and obtained a value of $y(1) = (2.8 \pm 0.3) \times 10^{-2}$ at room temperature using a low-pressure flow reactor interfaced with a mass spectrometer. A similar value was also determined for the uptake of HN03 by the NaNO3 powder and this result is surprising because these uptake mechanisms are apparently very different. These y values were based on the geometric area of the sample holder and were not corrected for internal surface areas of the substrates. The solid NaCl samples were prepared by grinding crystalline salt into a powder and typical grain sizes varied between 5 and 100 μm as determined by scanning electron microscopy. If we assume the average grain size is 20 μm and use our layer model [35,36], the corrected y value becomes $y(1) = 0.002\text{--}0.003$, significantly smaller than our present result at room temperature. It is possible that the partial HN03 pressures used in their experiments are greater than those used in ours, resulting in surface deactivation and, hence, a smaller observed y value.

In a study of reaction (2), Livingston and Finlayson-Pitts used an infrared spectrometer to monitor both the reactant (N_2O_5) and the product (ClNO_2); a lower limit of 2.5×10^{-3} at 298 K was estimated [16]. The N_2O_5 concentrate ion used was very large, about 1×10^{14} molecules/ cm^3 (or 3×10^{-3} Torr), which is several orders of

magnitude greater than atmospheric conditions. The observed γ value is significantly greater than the results listed in Table 2. The discrepancy is probably due to the estimation of the residence time, -0.16 s, for N₂O₅ over the NaCl. In their study gaseous N₂O₅ in 1 atm. air was expanded from a 5 L. bulb through NaCl packed in a cylindrical cell of cross sectional area 3.1 cm² and 20 cm length into a long pathlength infrared cell. The average flow rate was calculated from the pressure decrease in the 5 L bulb. It is rather unlikely that the gas mixture flowed through the NaCl column within such a short time unless a fast switching valve was used. Of course, this suggestion is very speculative and **further** work on reaction (2) may be necessary.

In a very recent study, George et al [20] studied the uptake of N₂O₅ by NaCl solutions from 262 to 278 K using a droplet train technique. The experimental conditions used are similar to those in the troposphere. They monitored the formation of nitrate in the liquid phase by ion chromatography and therefore the detection scheme is not selective for possible reaction products, ClNO₂ and HNO₃. A value of $\gamma(2)$ from 0.014 to 0.039, much larger than our data for dry salt, was reported because of the contribution from the N₂O₅ + H₂O reaction. They also determined the yield of ClNO₂ as a function of relative humidity using infrared spectroscopy [20].

Using a deposition profile in a laminar flow tube, in which the walls were coated with the NaCl substrates, Msibi et al. [21] obtained a value of 0.015 for 5% solution and < 0.002 for dry salts at 45-96% relative humidity. Ion chromatography was used to monitor the NO₃⁻ concentrations. The production of gas phase nitric acid on the surface followed by its absorption distorted the deposition profiles; hence a correction for this effect was required. Nonetheless, the results suggest the hydrolysis of N₂O₅ can be important, consistent with our findings discussed in the previous section.

implications for the Lower Stratosphere and Marine Troposphere. The implications of the heterogeneous reactions studied in this paper for the stratosphere are

investigated using the Caltech/JPL one-dimensional photochemical model. We shall focus on an explanation of the observed increase of HCl in the lower stratosphere after the El Chichon volcanic eruption in 1982 [3]. The details of the model are described by Michelangelo et al. [4]. The concentration of NaCl-containing aerosols is based on the observations of Woods et al. [2] and estimated by Michelangelo et al. [5]. The frequency of a reactive collision between a gas-phase molecule and NaCl is $J_{\text{NaCl}} = 1/4 \gamma \bar{v} A N_0$, where γ is the reaction probability, \bar{v} is the average speed of the impacting molecule ($\sqrt{8kT/\pi m}$), A is the surface area per particle, and N_0 is the number density of particles. Using the data given by Michelangelo et al. [5], we obtain a value of $J_{\text{NaCl}} = 1.14 \times 10^{-2} \gamma$ (s^{-1}) at 28 km. Since HN03 is the most abundant odd nitrogen species in the stratosphere, we shall first investigate the reaction between NaCl and HN03. If we adopt a value of $\gamma(1) = 8.0 \times 10^{-3}$ (from Table 1) for reaction (1), then we have $J_{\text{NaCl}} = 9.1 \times 10^{-5} \text{ s}^{-1}$. This implies that the time constant for the release of HCl from NaCl is of the order of hours. However, we believe that this sustained rate of release is unlikely because HN03 adsorbs on the surface of NaCl (see Figures 6a and b) and subsequent reaction may be limited by the rate of diffusion of HNO₃ through the solid aerosol. The product of the reaction between NaCl and HN03 is NaNO₃. It is unlikely that the latter will be released to the atmosphere. The accumulation of NaNO₃ on the aerosol surface reduces the efficiency of subsequent reactions between NaCl and HN03 as shown in Figure 6. Thus, we cannot adopt the straightforward value of $\gamma(1)$ from Table 1.

In modeling the time evolution of the release of HCl from reaction (1), we adopt a two-stage process, using a time-dependent γ value. In the first stage we allow the reaction to proceed with $\gamma = \gamma_0 e^{-t/\tau}$, where t is the time and τ is 30 minutes. The choice of 30 minutes is based on the following consideration. By this time we estimate that a fraction ($-1/e$) of the surface is covered by NaNO₃. With this parameterization of γ , its value would become small after about 100 minutes. In the second stage of our scheme we assume that the heterogeneous rate coefficient is slower by a factor of 100 due to

saturation of surface sites (the choice of this factor is based on our laboratory data shown in Figure 6 and we shall discuss the sensitivity of our model results to this choice). The model is allowed to run for 6 days. The initial profile of HCl and those after 6 hours and 6 days are presented in Figure 10a. The initial HCl profile is taken from the “standard” model of the stratosphere in 1982 with $\text{Cly} = 1.6$ ppb. The corresponding column density is $1.28 \times 10^{15} \text{ cm}^{-2}$. The column density of the profile after 6 hours is 8 % higher than the initial column density (see Figure 10b). At the end of 6 days the column density of HCl has increased to $1.88 \times 10^{15} \text{ cm}^{-2}$, or about 40 % greater than the initial value. This is in good agreement with the observations [3]. Note that the bulk of the increase is in the layer of enhanced aerosol concentrate ions [3, 4]. After this time the heterogeneous reaction is switched off (presumably due to the exhaustion of available NaCl), as further heterogeneous release of HCl will violate the observations of Mankin and Coffey [3]. The model is allowed to run for another 120 days. The main effect in this period is a gradual smoothing of the HCl profile due to eddy diffusion. Beyond 120 days the dispersion of the volcano-enhanced HCl in the atmosphere will be mostly due to the effects of horizontal motion and the one-dimensional model is no longer realistic. The time history of the HCl column density is given in Figure 10b.

The modeling results on the release of HCl from reaction (1) shown in Figure 10a and b obviously depend on the choice of two arbitrary parameters. The first is the choice of the time constant $\tau = 30$ minutes for the initial phase of reaction that coats the surface of the aerosol with HN03 and NaN03 . Since this time is so short compared with other atmospheric time constants, we may regard this phase as “instantaneous”. During the second phase of the interaction between NaCl and HN03 , we reduce its efficiency from the measured value by a factor of 0.01. The exact value of this reduction factor will affect the time constant for the reaction between NaCl and HN03 to reach saturation. For instance, if this factor were more than 0.01, release of HCl would terminate in less than 6 days. If this factor were 0.001, then the release of HCl would take 60 days. All these

cases would still be consistent with the available observations. ElChichon volcano erupted in March and April of 1982. The first observations that documented an increase of stratospheric HCl were taken in July 1982 [3]. This is more than 60 days after the eruption. It is clear that to narrow down the range of uncertainty in the release rate of HCl from NaCl further laboratory experiments as well as timely volcanic observations must be carried out.

There are three other reactions that are capable of releasing HCl from NaCl in the stratosphere, involving N₂O₅, ClONO₂ and NO₂ (reactions 2-4). However, the concentrations of the latter species in the lower stratosphere are much smaller than that of HN₃ and their values for reactions (2) - (4) are smaller than that for reaction (1). Hence, they will not be able to competitively react with NaCl, especially after all the surface sites are occupied by HN₃ or NaN₃. Even if these reactions are competitive, they will just add to the production of HCl, although the time constant for the appearance of HCl would be different. The main difference between reaction (1) and reactions (2-4) is that the former releases HCl directly, whereas the latter release chlorine in labile forms, such as ClONO₂, Cl₂ or NOCl. The most likely fate of these molecules is removal by photodissociation, releasing Cl atoms. The conversion of Cl to HCl proceeds by the reaction



This reaction by itself will remove Cl in the lower stratosphere with a time constant of the order of 100 seconds. However, the bulk of Cl atoms will preferentially react with O₃ rather than with CH₄. Taking this into account implies that the conversion of active chlorine to HCl takes about 10 days in the lower stratosphere. Thus, the overall result of reactions (2-4) are the same as that for reaction (1), with the time constant being the only difference.

In summary, we conclude that the measured reaction probability between NaCl and HN03 reported in this work provides an adequate explanation of the observed increase of HCl after the ElChichon eruption.

The implications of the heterogeneous reactions studied in this paper for tropospheric chemistry will now be briefly discussed. HCl has been detected in the marine troposphere with concentrations of the order 100 to 1000 pptv (see [38] and references cited therein). By comparison, the gas phase chemistry predicts only about 10 pptv, consistent with the HCl profile shown in Figure 10 when extrapolated to the troposphere. Reaction (1) has been postulated to release HCl from NaCl. The most compelling evidence in support of this mechanism is the recent measurement of HCl by Eldering et al. [12] in coastal Southern California. The concentrations of HCl ranged from 39 to 1250 pptv and appeared to correlate with similar concentrations of HN03. We may roughly estimate the time constant for the interaction between NaCl and HN03 as follows. The aforementioned experiment reported concentrations of $6.3 \mu\text{g}/\text{m}^3$ of NaCl. Assuming an average radius of $1 \mu\text{m}$, we estimate a collision frequency of $J_{\text{NaCl}} = 1 \times 10^{-5} \text{ s}^{-1}$, where a value of γ of 1.3×10^{-2} has been taken from Table 1. At this rate, the conversion of NaCl to HCl occurs in one day and is fast enough to account for the observed HCl concentrations. Reactions (2) and (3) can contribute to the production of HCl, but will be less important due to the lower concentrations of N2O5 and ClONO2 and smaller γ values (see Table 1).

Acknowledgment. The research described in this article was performed at the Jet Propulsion Laboratory, California Institute of Technology, under a contract with the National Aeronautics and Space Administration. YLY acknowledges support of NASA grant NAGW 2204 to the California Institute of Technology. The authors are grateful to Veronica Bierbaum and Carleton Howard for helpful discussion on the development of CIMS, Renyi Zhang for the design of the data acquisition system, and Greg Huey for sending the preprint.

References and Notes

1. Solomon, S. *Nature* **1990**, **347**, 347.
2. Woods, D. C.; Chuan, R. L.; Rose, W. I. *Science* **1985**, **230**, 170.
3. Mankin, W. G.; Coffey, M. T. *Science* **1984**, 226, 170.
4. Michelangelo, D. V.; Allen, M.; Yung, Y. L. *J. Geophys. Res.* 1989, 94, 18429.
5. Michelangelo, D. V.; Allen, M.; Yung, Y. L. *Geophys. Res. Lett.* **1991**, **18**, 673.
6. Finlayson-Pitts, B. J. *Nature* **1983**, 306, 676.
7. Finlayson-Pitts, B. J.; Ezell, M. J.; Pitts, J. N., Jr. *Nature* 1989, 337, 241.
8. Keene, W. C.; Pszenny, A. A. P.; Jacob, D. J.; Duce, R. A.; Galloway, J. N.; Schultz-Tokos, J. J.; Sievering, H.; Boatman, J. F. *Global Biogeochem. Cycles* 1990, 4, 407.
9. Pszenny, A. A. P.; Keene, W. C.; Jacob, D. J.; Fan, S.; Maben, J. R.; Zetwo, M, P.; Springer-Young, M.; Galloway, J. N. *Geophys. Res. Lett.* 1993, 20, 699.
10. Cadle, S. H.; Countless, R. J.; Kelly, N. A. *Atmos. Environ.* 1980, 16, 2501.
11. Solomon, P. A.; Salmon, L. G.; Fall, T.; Cass, G. R. *Environ. Sci. Technol.* 1992, 26, 1594.
12. Eldering, A.; Solomon, P. A.; Salmon, L. G.; Fall, T.; Cass, G. R. *Atmos. Environ.* **1991**, **25**, 2091.
13. Galasyn, J. F.; Tschudy, K. L.; Hubert, B. J. *J. Geophys. Res.* 1987, 92, 3105.
14. Laux, J. M.; Hemminger, J. C.; Finlayson-Pitts, B. J. *Geophys. Res. Lett.* **1994**, **21**, 1623.
15. Fenter, F. F.; Caloz, F.; Rossi, M. J. *J. Phys. Chem.* 1994, 98, 9801.
16. Livingston, F. E.; Finlayson-Pitts, B. J. *Geophys. Res. Lett.* 1991, 18, 17.
17. Behnke, W.; Kruger, H.-U.; Scheer, V.; Zetzsch, C. *J. Aerosol Sci.* 1991, 22, S609; *ibid*, 1992, 23, S933.
18. Behnke, W.; Scheer, V.; Zetzsch, C. *J. Aerosol Sci.* 1993, 24, S115.

19. Zetzsch, C.; Behnke, W. *Ber. Bunsenges. Phys. Chem.* **1992**, 96,488.
20. George, Ch.; Ponche, J. L.; Mirabel, Ph.; Behnke, W.; Scheer, V.; Zetzsch, C. J. *Phys. Chem.* **1994**,98, 8780.
21. Msibi, I. M.; Li, Y.; Shi, J. P.; Harrison, R. M. *J. Atmos. Chem.* **1994**, 18,291.
22. Timonen, R. S.; Chu, L. T.; Leu, M. T.; Keyser, L. F. *J. Phys. Chem.* **1994**, 98, 9509.
23. Vogt, R.; Finlayson-Pitts, B. J. *J. Phys. Chem.* **1994**, 98,3747.
24. Chu, L. T.; Leu, M.-T.; Keyser, L. F. *J. Phys. Chem.* **1993**, 97, 7779.
25. Chu, L. T.; Leu, M.-T.; Keyser, L. F. *J. Phys. Chem.* **1993**, 97, 12798.
26. Gleason, J. F.; Sinha, A.; Howard, C. J. *J. Phys. Chem.* **1987**,91, 719.
27. Huey, L. G.; Hanson, D. R.; Howard, C. J., submitted to the Journal of Physical Chemistry (1994).
28. Davidson, J. A.; Viggiano, A. A.; Howard, C. J.; Dotan, I.; Fehsenfeld, F. C.; Albritton, D. L.; Ferguson, E. E. *J. Chem. Phys.* **1978**, 68, 2085.
29. Fehsenfeld, F. C.; Howard, C. J.; Schmeltekopf, A. L. *J. Chem. Phys.* **1975**, 63, 2835.
30. Gregg, S. J.; Sing, K. S. W. *Adsorption, Surface Area and Porosity*, Academy Press, New York (1982).
31. Weast, R. C. *Handbook of Chemistry and Physics*, CRC Press, 65th Edit ion (1984).
32. Walker, R. E. *Phys. Fluids* **1961**,4, 1211.
33. Kaufman, F. *Prog. React. Kinet.* **1961**, 1, 1.
34. Marrero, T. R.; Mason, E. A. *J. Phys. Chem. Ref. Data*, **J** **972**, 1, 3.
35. Keyser, L. F.; Moore, S. B.; Leu, M.-T. *J. Phys. Chem.* **1991**, 95, 5496.
36. Keyser, L. F.; Leu, M.-T.; Moore, S. B. *J. Phys. Chem.* **1993**,97,2800.
37. Satterfield, C. N. *Heterogeneous Catalysis in Industrial Practice*, Second Edition, McGraw-Hill, Inc. (1991).

38. Singh, H. B.; Kasting, J. F. *J. Atmos. Chem.* 1988, 7, 261.

Table 1. Summary of the reaction probability measurements for the $\text{HN03} + \text{NaCl} \rightarrow \text{HCl} + \text{NaN03}$ reaction. The total pressure is about 0.45 Torr in all experiments.

<u>p(HNO₃)</u>	<u>m(NaCl)</u>	<u>T</u>	<u>v</u>	<u>ks</u>	<u>kg</u>	<u>yg</u>	<u>yt</u>	<u>p(H₂O)</u>	<u>Notes</u>
Torr	g	K	cm/s	1/s	1/s			Torr	
7.9(-8)	22	295	2738	322	337	.069	.015	<2(.5)	a
1. 1(-7)	22	293	2756	337	353	.072	.016	1.8(-4)	c
1. 1(-7)	22	294	2699	303	317	.065	.014	<2(-5)	a
1.2(-7)	22	295	2828	380	400	.082	.019	2. 1(-4)	c
1.2(-7)	22	294	2721	347	365	.074	.016	1.5(-4)	c
1.4(-7)	22	295	2767	380	401	.082	.019	8.1(-5)	c
2.6(-7)	20	292	2445	289	304	.062	.013	<2(-5)	a
2.9(-7)	18	296	2346	276	291	.059	.012	<2(-5)	a
3. 1(-7)	20	295	2342	306	321	.065	.014	<2(-5)	b
3.4(-7)	20	295	1977	263	282	.056	.011	<2(-5)	a
4.0(-7)	18	294	2345	256	269	.055	.011	<2(-5)	a
6.0(-7)	20	297	2188	194	204	.042	.007	<2(-5)	a
6.4(-7)	20	294	1844	220	231	.047	.008	<2(-5)	a
1. 1(-6)	20	294	2124	178	187	.038	.006	<2(-5)	b
Average						Value =	.0133.004		
6.5(-8)	20	223	2114	182	187	.044	.008	<2(-5)	a
6.9(-8)	20	223	1728	134	138	.032	.005	<2(.5)	a
7. 1(-8)	20	223	2282	189	195	.046	.008	<2(-5)	a
7. 1(-8)	22	223	2311	229	236	.055	.011	1.5(-4)	c
7.3(-8)	20	223	2342	193	199	.047	.008	<2(-5)	a

8.3(-8)	22	223	2229	283	291	.068	.015	<2(-5)	a
9.2(-8)	22	223	2252	208	214	.050	.009	<2(-5)	a
9.7(-8)	20	223	1797	192	198	.047	.008	1.2(-4)	c
9.7(-8)	22	223	2312	211	217	.051	.010	1.1(-4)	c
1.0(-7)	20	223	2169	181	186	.044	.008	9.5(-5)	c
1.2(-7)	20	223	2171	211	217	.051	.008	<2(-5)	b
1.2(-7)	20	223	2191	239	246	.058	.012	1.6(-4)	c
1.3(-7)	20	223	2113	206	212	.050	.009	<2(-5)	a
1.3(-7)	20	223	1757	109	112	.026	.003	<2(-5)	a
1.4(-7)	20	223	2220	213	219	.051	.008	1.8(-4)	c
1.4(-7)	20	223	2104	115	118	.028	.004	1.4(-4)	c
Average						Value =	.008±.003		d

Notes:

- a. NaCl substrates were baked overnight in vacuum.
- b. NaCl substrates were not baked, but evacuated for about one hour.
- c. NaCl substrates were not baked and water vapors were admitted into the flow-tube reactor.
- d. This *value should* be considered as a lower limit. See text for details.

Table 2. Summary of the reaction probability measurements for the $\text{N}_2\text{O}_5 + \text{NaCl} \rightarrow \text{ClNO}_2 + \text{NaNO}_3$ reaction.

<u>NaCl Substrates</u>	<u>T = 296 K</u>	<u>Number of Experiments</u>	<u>T = 223 K</u>	<u>Number of Experiments</u>
Baked a)	$< 1.0 \times 10^{-4}$	4	$< 1.0 \times 10^{-4}$	3
Unbaked (b)	$\approx 4.5 \times 10^{-4}$	4	$\approx 2.4 \times 10^{-4}$	6

Notes:

- a. NaCl substrates were baked overnight in vacuum.
- b. NaCl substrates were not baked, but evacuated for about one hour. The enhancement of the reaction probability is due to the $\text{N}_2\text{O}_5 + \text{H}_2\text{O} \rightarrow 2 \text{HNO}_3$ reaction on the surfaces of the NaCl granules.

Table 3. Reaction probabilities for heterogeneous reactions involving NaCl: comparison with previous measurements

<u>Reaction</u>	<u>Reaction Probability</u>	<u>Temperature</u>	<u>Substrate Condition</u>	<u>Reference</u>
HN03 + NaCl	1.3×10^{-2}	296 K	dry or slightly wet	this work
	$>8.0 \times 10^{-3}$	223 K	dry or slightly wet	this work
	4.0×10^{-4}	298 K	dry	Laux et al.[14]
	$2.8 \times 10^{-2(a)}$	298 K	dry	Fenter et al.[15]
N ₂ O ₅ + NaCl	$<1.0 \times 10^{-4}$	296 K	dry	this work
	$<1.0 \times 10^{-4}$	223 K	dry	this work
	$\approx 4.5 \times 10^{-4}$	296 K	slightly wet	this work
	$\approx 2.4 \times 10^{-4}$	223 K	slightly wet	this work
	$>2.5 \times 10^{-3}$	298 K	dry	Livingston and Finlayson-Pitts[16]
	0.014-0.039	263-278 K	solution	George et al.[20]
	$<2.0 \times 10^{-3}$	298 K	wet	Msibi et al.[21]
ClONO ₂ + NaCl	4.6×10^{-3}	296 K	dry or slightly wet	Timonen et al.[22]
	6.7×10^{-3}	225 K	dry or slightly wet	Timonen et al.[22]
N ₂ O + NaCl	$6 \times 10^{-5} - 5 \times 10^{-8}$	298 K	dry	Vogt and Finlayson-Pitts[23]

Note: (a) The y value, corrected for internal surface areas, is about 0.002-0.003.

Figure Captions

Figure 1. Schematic diagram of the neutral flow-tube reactor coupled to a chemical ionization mass spectrometer (**CIMS**). The bottom of the reactor was recessed and made flat in order to hold the **NaCl** substrates in place. See Figure 2 for details.

Figure 2. End view and side view of the flow-tube reactor. See text for details.

Figure 3. Calibration of **HN03** signals as a function of concentration. The total pressure is 0.349 Torr and the temperature is 296 K.

Figure 4. Calibration of **N205** signals as a function of concentrations. The total pressure is 0.431 Torr and the temperature is 296 K.

Figure 5. Uptake of **HN03** by **NaCl** at 296 K. Both the **HNO₃** loss and **HCl** growth are monitored. (a) for reaction time up to 18 minutes and (b) for reaction time as long as 3 hours.

Figure 6. (a) Uptake of **HN03** by **NaCl** at 223 K. Both physical adsorption and heterogeneous reaction are evident. (b) Physical uptake of **HNO₃** by **NaN03** at 223 K.

Figure 7. The loss of **HN03** signals as a function of injector position at 295 K. Open circles for data obtained from the injector moving from downstream to upstream. Closed circles for data obtained from the injector from upstream to downstream. See text for details.

Figure 8. The loss of HN03 signals as a function of injector position at 223 K. **Open** circles for data obtained from the injector moving from downstream to upstream. Closed circles for data obtained from the injector moving from upstream to downstream. See text for details.

Figure 9. Loss of N205 as a function of injector position. Solid circles for a blank experiment with no NaCl present. Open circles for data in the presence of NaCl .

Figure 10. (a) Time dependent profile showing the evolution of HCl as computed by the **Caltech/JPL** one-dimensional photochemical model. The standard profile (a) is given for time = 0. The profiles (b), (c) and (d) refer to the time of 6 hours, 6 days and 120 days, respectively. (b) Time dependent column density of HCl as computed by the **Caltech/JPL** one-dimensional photochemical model. See text for further details.

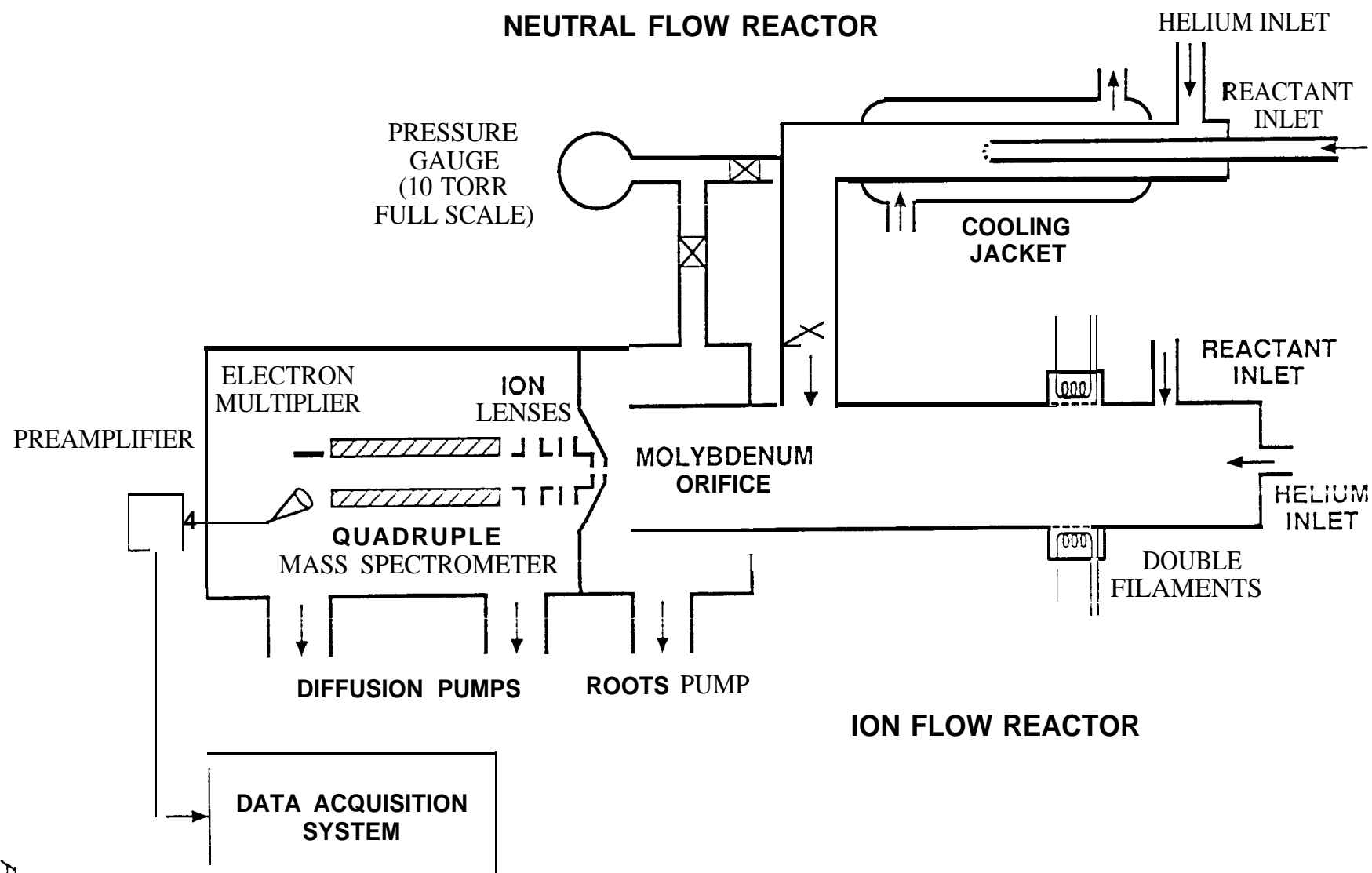


Fig 1

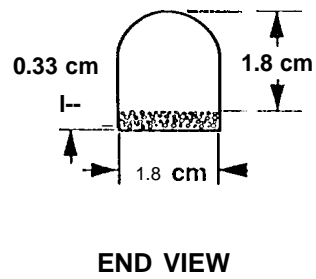
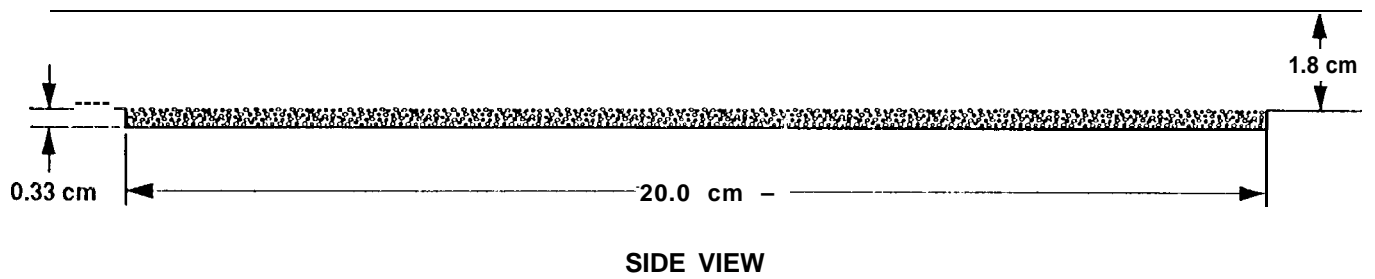
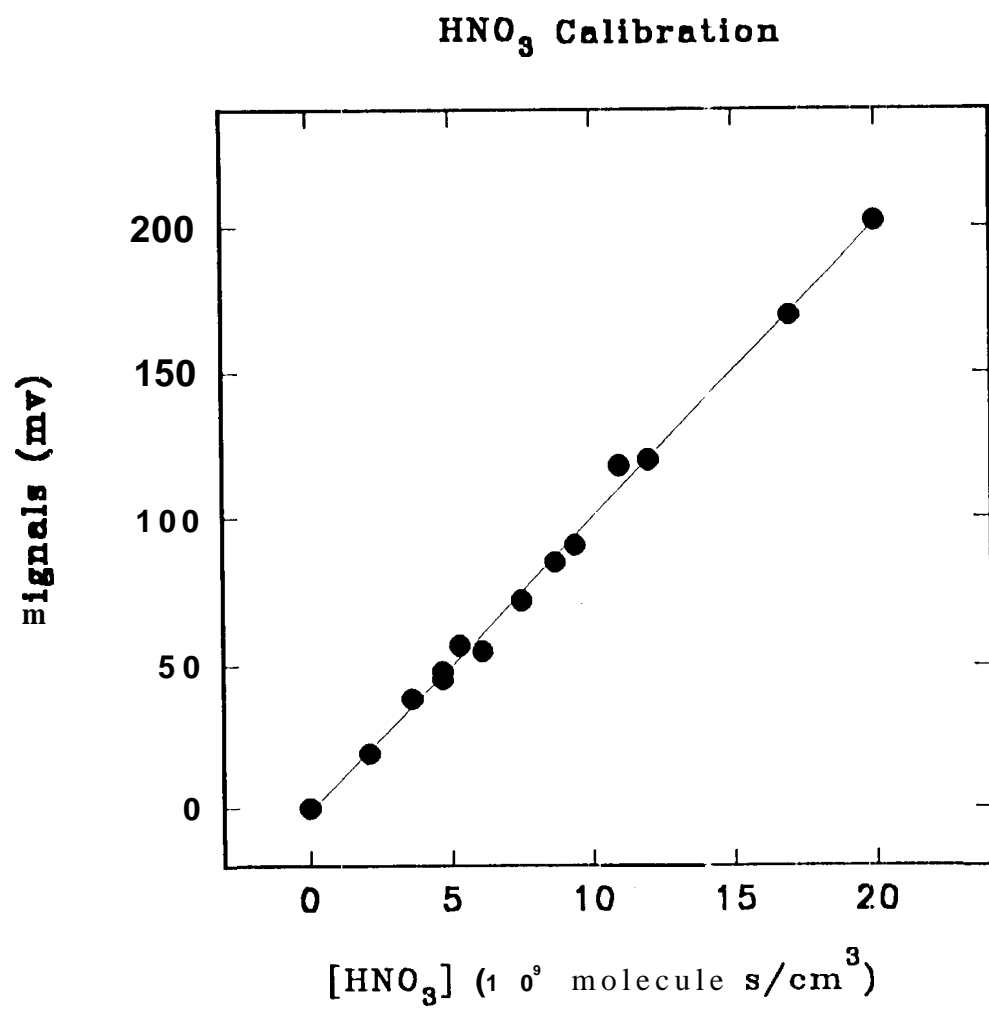


Fig. 2



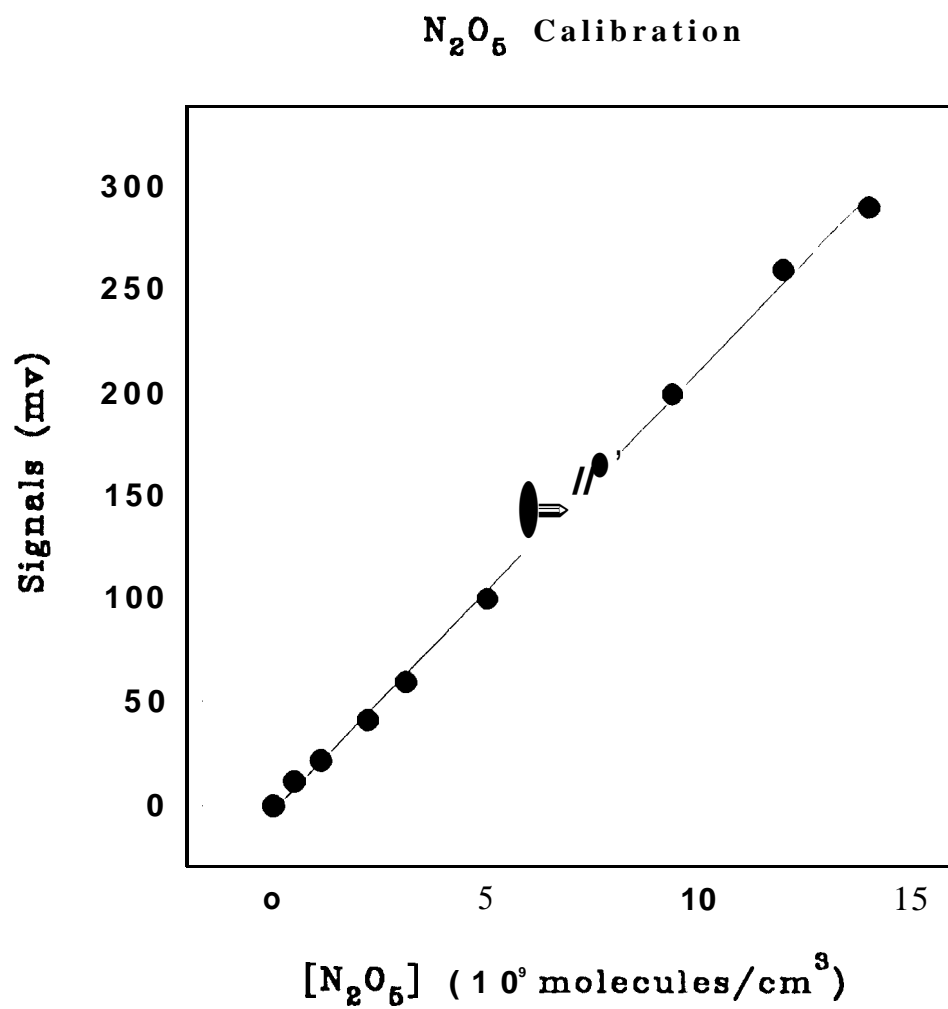


Fig. 4

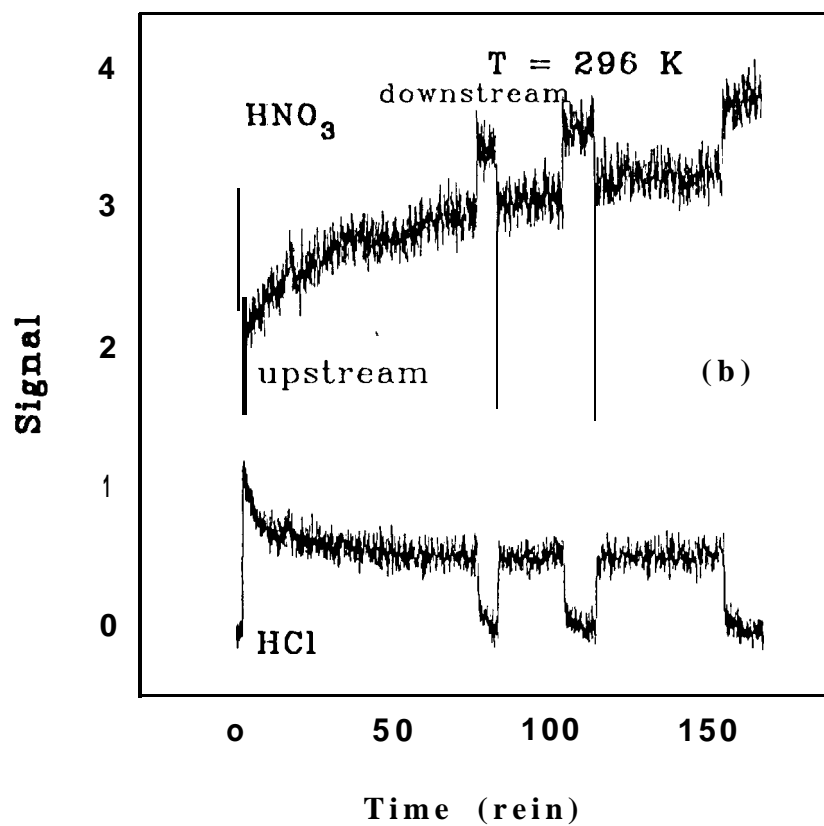
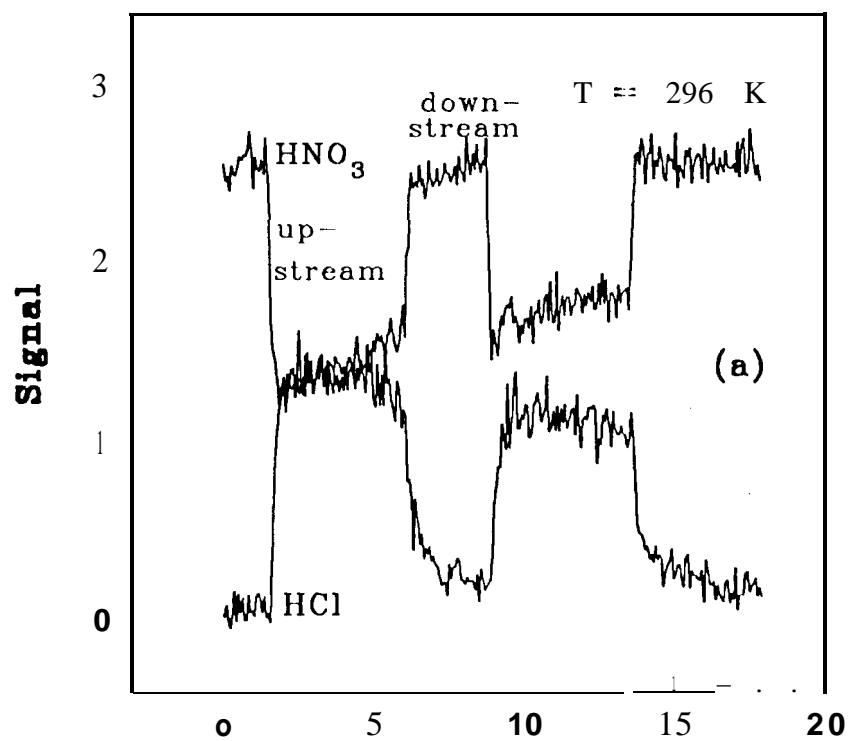
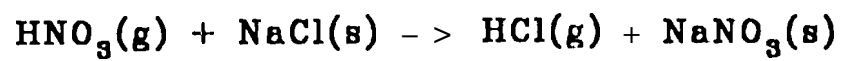
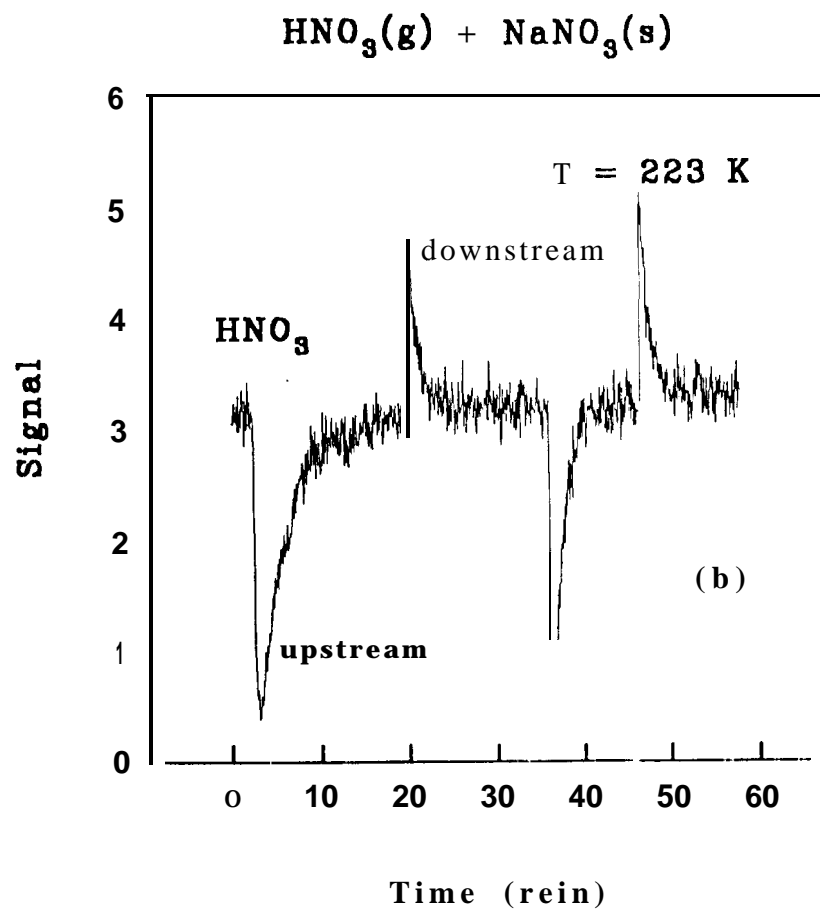
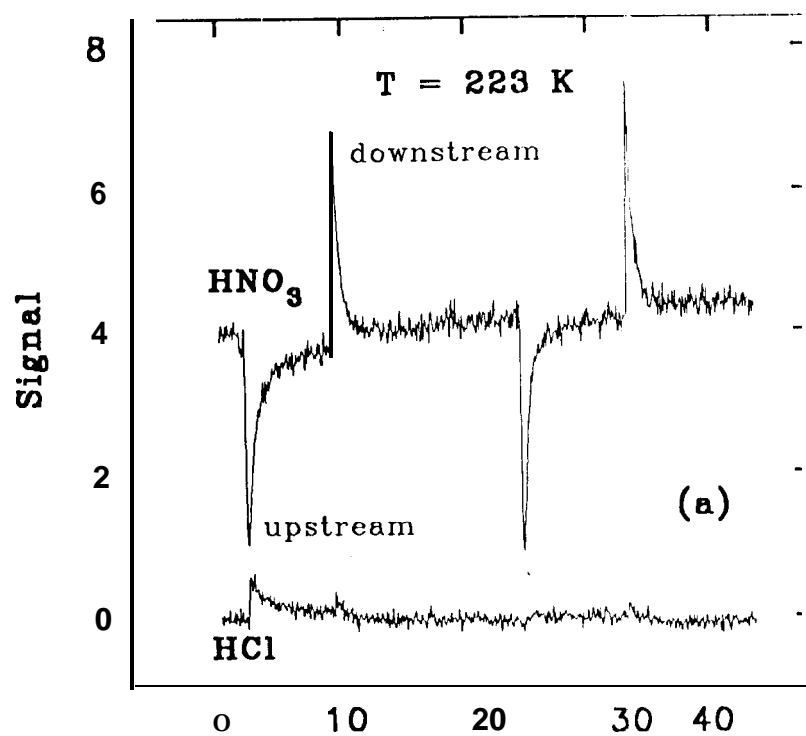
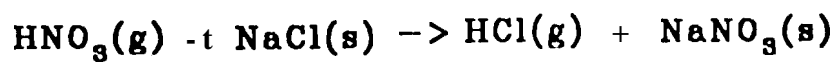


Fig. 5



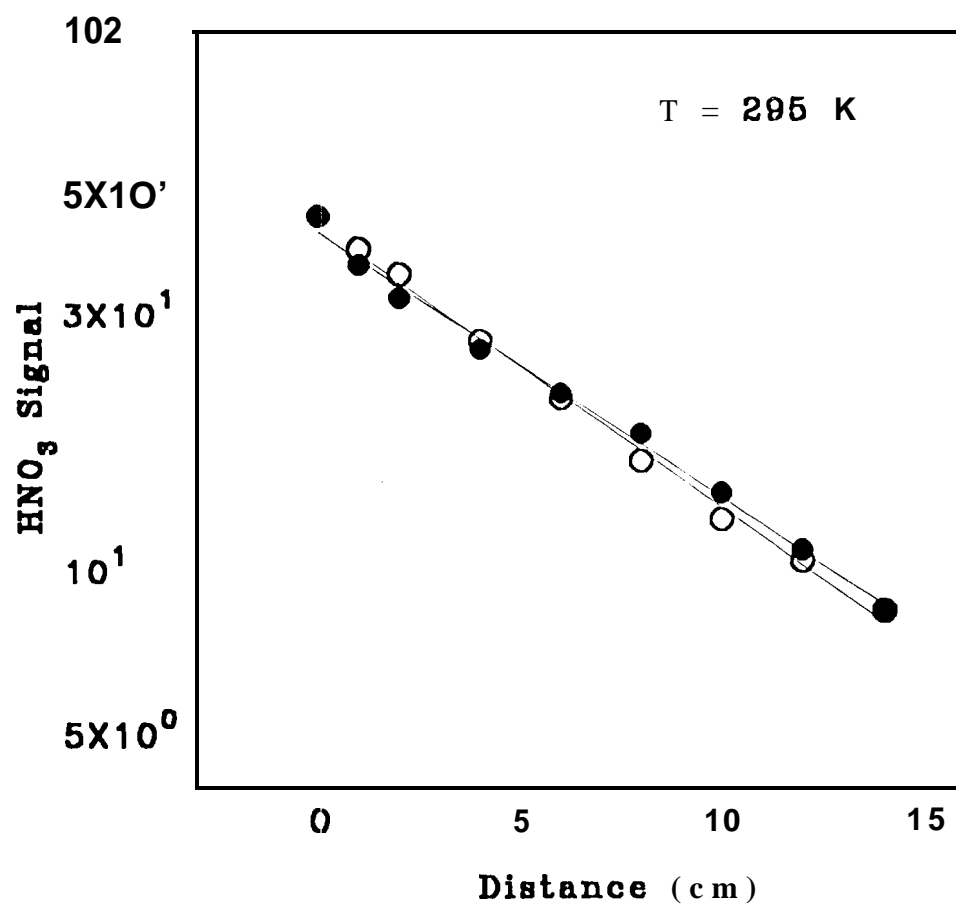
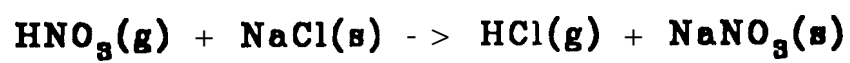


Fig. 7

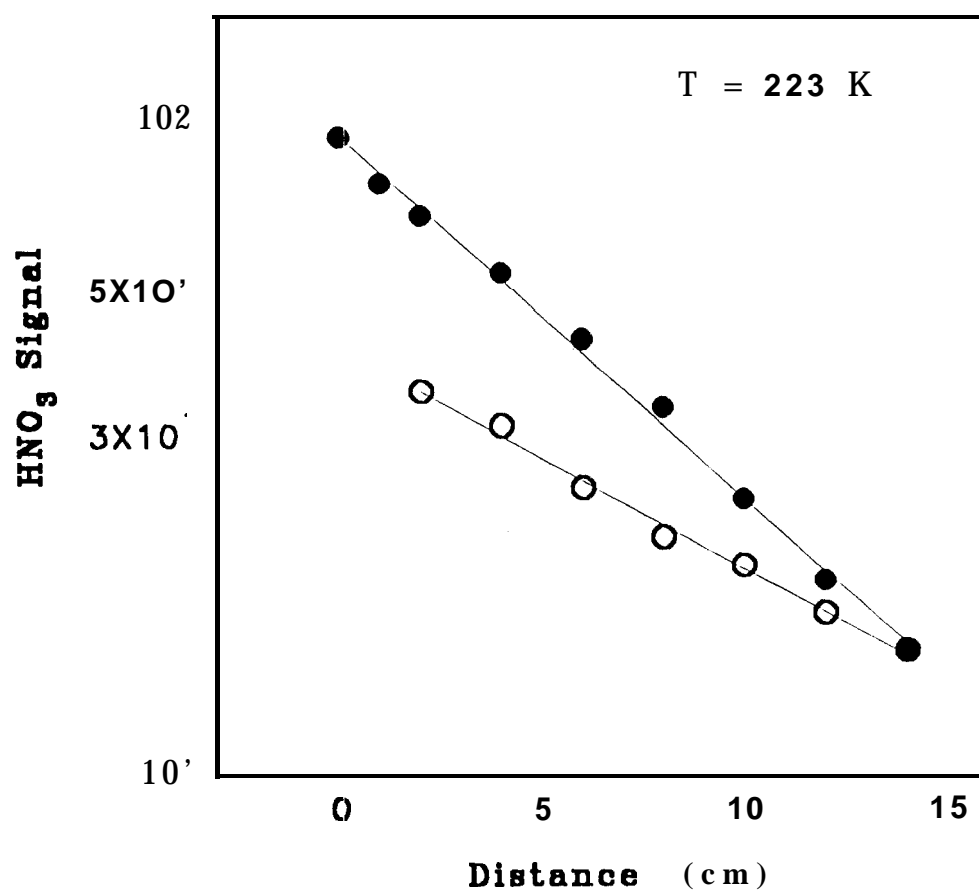
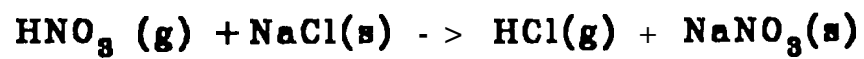
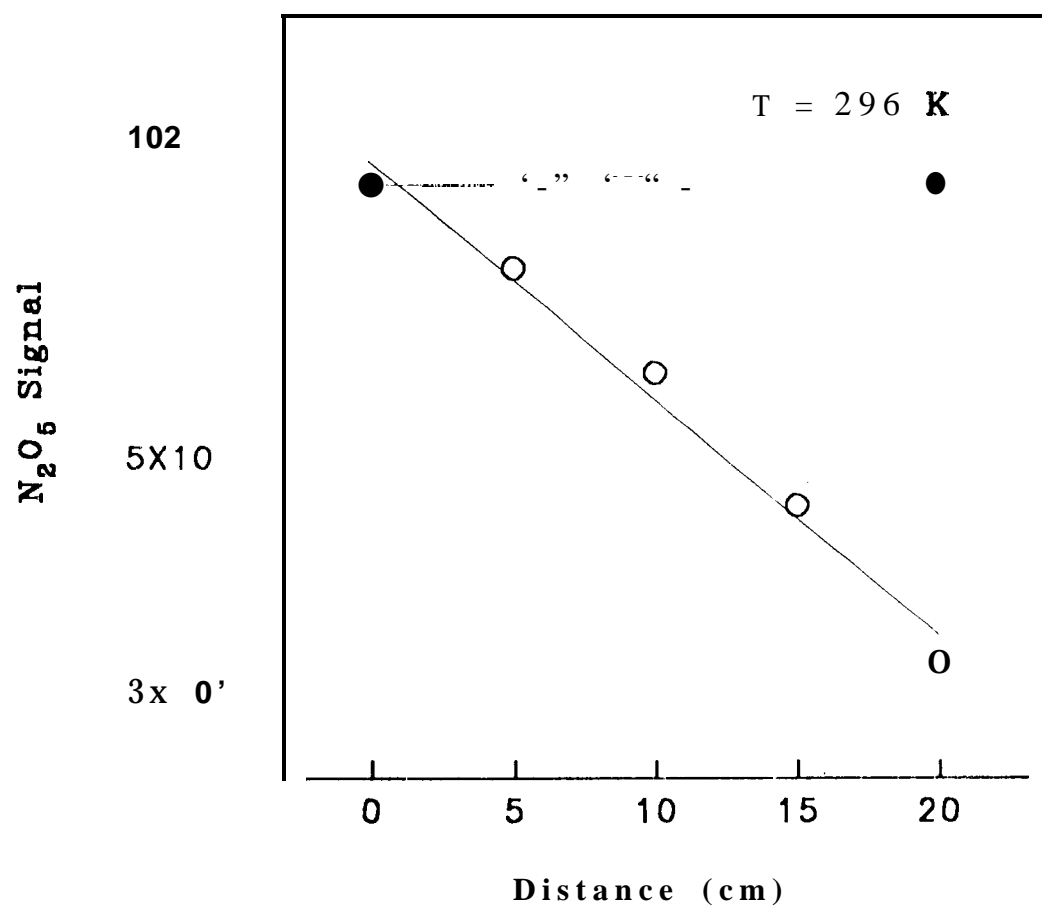
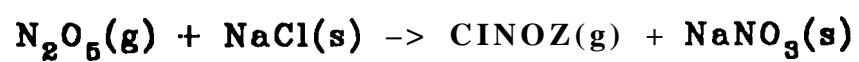


Fig. 8



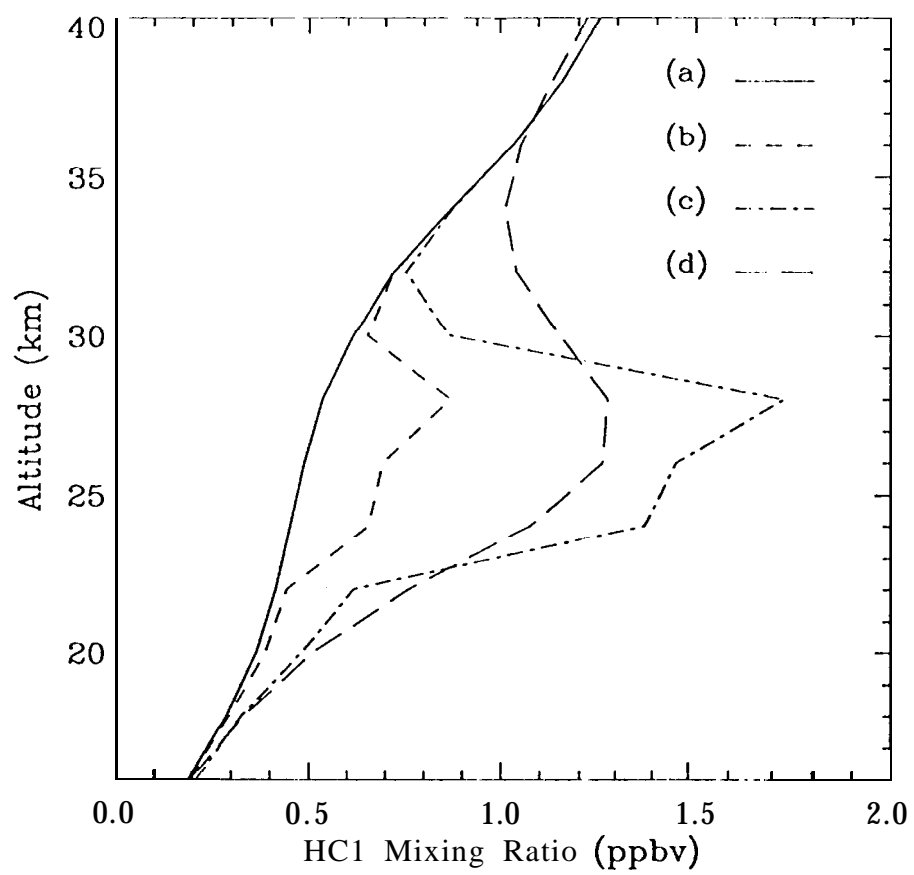


Fig. 10(a)

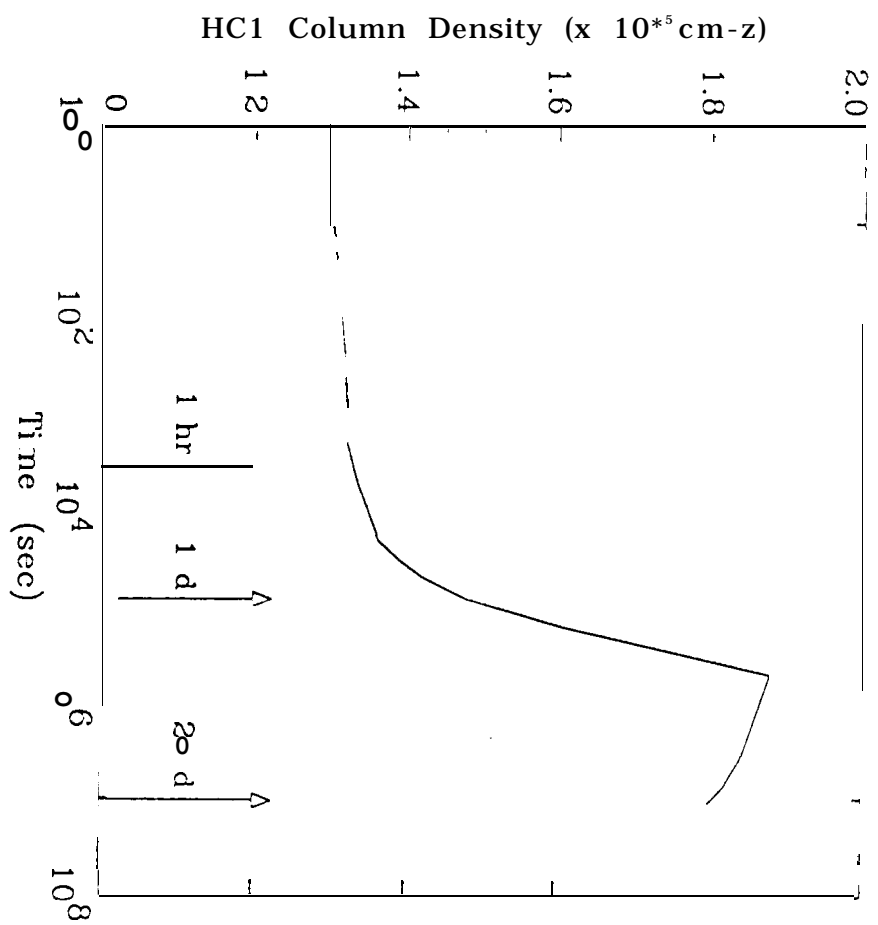


Fig. 1006